Basicity properties of two paracyclophane receptors. Their ability in ATP and ADP recognition in aqueous solution

Carla Bazzicalupi,[a] Andrea Bencini,*[,a] Antonio Bianchi,*[,a] Vieri Fusi,[b] Claudia Giorgi,[a] Andrea Granchi,[a] Piero Paoletti*[,a] and Barbara Valtancoli[a]

[a] *Department of Chemistry, University of Florence, via Maragliano 75/77, 50144 Florence, Italy*
[b] *Institute of Chemical Sciences, University of Urbino, Piazza Rinascimento 6, 61029, Urbino, Italy*

The protonation behaviour of the aza-cyclophane receptor 6,13,15,18-tetramethyl-6,13,15,18-tetraaza-1(1,4),11(1,4)-dibenzena-3(1,4),9(1,4)-dipiperazina-cyclodecanonaphane (L2) has been studied in aqueous solution by means of potentiometric and ^{1}H and ^{13}C NMR techniques. L2 behaves as a hexaprotic base and NMR experiments allow the determination of the stepwise protonation sites. Considering the $[H_5L2]^{5+}$ species, the acidic protons occupy alternate positions in the macrocycle, separated by an unprotonated amino group or by a *p*-phenylene moiety. The crystal structure of $[H_5L2](ClO_4)_5\cdot1.5H_2O$ (space group $P\bar{1}$, a = 8.87(1), b = 15.388(6), c = 20.476(7) Å, α = 102.80(3)°, β = 93.43(5)°, γ = 101.41(6)°, V = 2656(3) Å^3, Z = 2, R = 0.0803) confirms the NMR data, showing one proton located on the N(1) methylated nitrogen and four protons on the amino groups adjacent to the aromatic rings. These features are analogous to those found in the paracyclophane L1, which shows a similar molecular architecture. Binding of ATP and ADP by L1 and L2 was studied by means of potentiometry and ^{31}P NMR in aqueous solution. Although the $[H_4L1]^{4+}$ and the $[H_5L2]^{5+}$ species show a similar charge distribution, $[H_4L1]^{4+}$ forms stable complexes with ATP and ADP, while $[H_5L2]^{5+}$ does not bind such nucleotides. These results may be explained considering the different orientation of the N–H$^+$ bonds in the two receptors.

Selective recognition of guest molecules by synthetic receptors through the formation of hydrogen bonds has been extensively analysed in the last few years. Such studies have been performed mainly in lipophilic solvents because of the strong solvation of the interacting groups in polar media.[1–3]

The design of host molecules for recognizing anions, such as carboxylic acids or nucleotides, in aqueous solution is an important target in view of the biological relevance of studies in this solvent.[4–10] This goal is not easily achieved as strong solvent–guest interactions can efficiently compete with the process of selective complexation. However, polyammonium macrocycles may behave as efficient receptors for polycharged anions in aqueous solution.[4–14] Preorganization of the macrocyclic host and spatial charge matching have been recognized as primary conditions for strong host–guest interactions. In addition to charge–charge interactions, stacking and solvophobic forces acting on the nucleobases and hydrogen bonds between anionic functions and polyamine receptors can furnish additional contributions to complex stabilization.[5,12,13,15,16]

Previously, we reported the synthesis and basicity properties of the macrocycle **L1**.[17] Protonation of **L1** occurs on the benzylic nitrogens and results in the formation of an $[H_4L1]^{4+}$ species, which is present in solution in a wide pH range.

In this paper we report the synthesis and protonation behaviour of the paracyclophane 6,13,15,18-tetramethyl-6,13,15,18-tetraaza-1(1,4),11(1,4)-dibenzena-3(1,4),9(1,4)-dipiperazina-cyclodecanonaphane (**L2**).

The macrocycles **L1** and **L2** present a similar molecular architecture, composed of two polyamine subunits linked by aromatic spacers (Fig. 1). The presence of aromatic moieties, the short ethylenic chains connecting the amine groups, nitrogen methylation and, in **L2**, the piperazine rings, give rise to rigid macrocyclic frameworks. The coordination of anionic guests can be achieved by using, as host species, polyprotonated forms of aza-paracyclophanes.[13] In order to test the binding properties of such preorganized receptors toward anionic species, we have analysed their ability in ATP and ADP recognition. The basicity properties of such receptors are strictly related to their

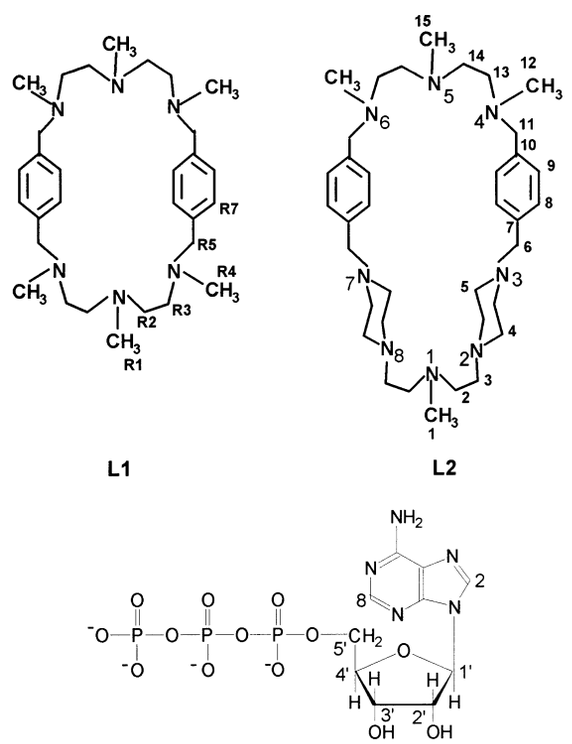

Fig. 1 Ligands and ATP drawing with labelling employed in ^{1}H and ^{13}C NMR assignments

binding features and the study of their proton transfer behaviour is a key step in the analysis of the binding characteristics toward anionic species. As a consequence, the stepwise protonation equilibria of **L2** have been studied by means of potentiometric and ^{1}H and ^{13}C NMR techniques and the results are reported herein. The crystal structure of the $[H_5L2](ClO_4)_5\cdot1.5H_2O$ salt adds further information about the protonation behaviour of **L2**.

Table 1 Protonation constants (log K) of **L1** and **L2** determined by means of potentiometric measurements in 0.15 mol dm^{-3} NaCl aqueous solution at 298.1 K

	L1 log K	**L2**
$\mathbf{L} + H^+ = \mathbf{L}H^+$	8.93[a]	9.81(3)[b]
$\mathbf{L}H^+ + H^+ = \mathbf{L}H_2^{2+}$	8.22	8.67(2)
$\mathbf{L}H_2^{2+} + H^+ = \mathbf{L}H_3^{3+}$	7.35	7.84(3)
$\mathbf{L}H_3^{3+} + H^+ = \mathbf{L}H_4^{4+}$	6.44	6.65(3)
$\mathbf{L}H_4^{4+} + H^+ = \mathbf{L}H_5^{5+}$	1.5	6.11(3)
$\mathbf{L}H_5^{5+} + H^+ = \mathbf{L}H_6^{6+}$	—	2.78(4)

[a] From ref. 17(*a*). [b] Values in parentheses are standard deviations on the last significant figure.

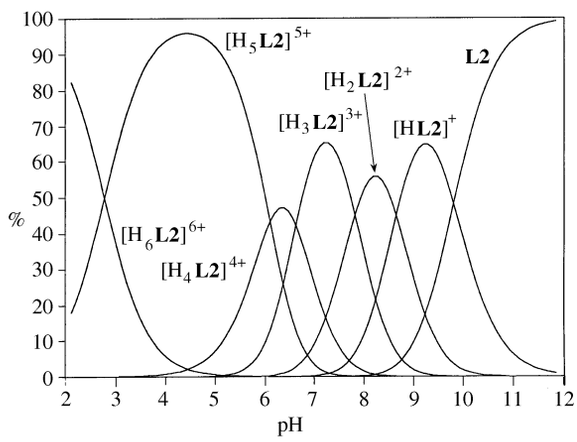

Fig. 2 Distribution diagram of the protonated species formed by **L2** as a function of pH ([**L2**] = 1 × 10^{-2} mol dm^{-3}) at 298 K

Results and discussion

Protonation of L2

The protonation equilibria of **L2** have been studied in 0.15 mol dm^{-3} NaCl solution at 298.1 ± 0.1 K by potentiometric pH (−log [H$^+$]) measurements. The protonation constants are reported in Table 1, together with those of **L1**. The distribution diagram for the species present in solution as a function of pH for the system **L2**/H$^+$ is reported in Fig. 2.

L2 behaves as a hexaprotic base in the pH range investigated (2.5–11). The first five basicity constants range between 9.81 and 6.11 logarithmic units, while the sixth one is less than 3 logarithmic units and further protonation steps are not detectable by means of potentiometry in aqueous solution. This behaviour can be rationalized considering the minimization of electrostatic repulsion between positive charges in protonated species of polyaza macrocycles. In other words, the first five protons can occupy alternate positions in the macrocycle, separated by one unprotonated nitrogen or *p*-phenylene units, while in the hexaprotonated receptor three or more protonated nitrogens are necessarily contiguous. As a consequence, $[H_5\mathbf{L2}]^{5+}$ is the species largely prevalent in aqueous solution in a wide pH range (pH 3–6, see Fig. 2). These considerations are supported by the NMR study in aqueous solution and the crystal structure of the $[H_5\mathbf{L2}]^{5+}$ cation, which shows the five protons located on the N(3), N(4), N(6), N(7) and N(1) nitrogen atoms (*vide infra*).

The protonation constants of **L1** and **L2** are compared in Table 1. Even if **L2** can bind up to six protons in aqueous solution, the two macrocycles show a similar protonation behaviour. In particular, the first four basicity constants of **L1** are much higher than the fifth one. This behaviour has been explained considering that in the tetraprotonated $[H_4\mathbf{L1}]^{4+}$ species the four protons are located on the benzylic nitrogens, both in solution and in the solid state.[17a] Such a disposition minimizes the repulsion between positive charges, resulting in a stabilization of the $[H_4\mathbf{L1}]^{4+}$ species which is prevalent in aqueous solution in a wide pH range (pH 2.5–6.5).

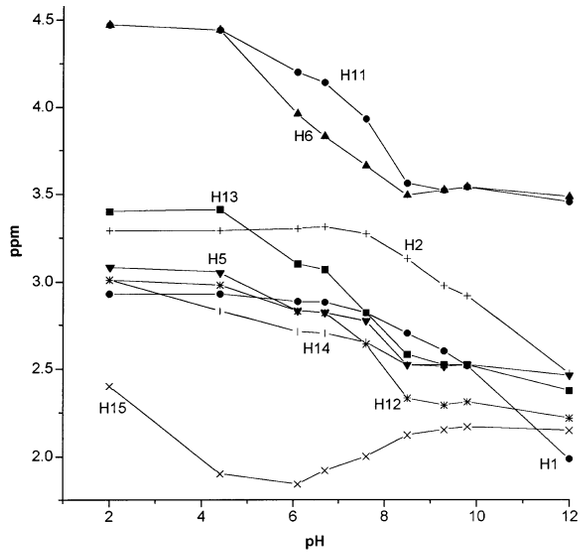

Fig. 3 Experimental ^{1}H chemical shifts of **L2** as a function of pH. (The signals of the aromatic protons, as well as those of the protons H3 and H4, have been omitted for clarity. Their chemical shifts do not change significatively in the pH range investigated.)

In order to shed further light on the protonation mechanism of **L2**, ^{1}H and ^{13}C NMR spectra in aqueous solution have been recorded at various pH values. All the assignments have been made on the basis of ^{1}H–^{1}H homonuclear and ^{1}H–^{13}C heteronuclear correlation experiments at the different pH values studied.

Table 2 reports the ^{1}H and ^{13}C chemical shift for **L2** at pH 11.6, where the unprotonated amine predominates in solution; the spectral features account for a C_{2v} time-averaged symmetry. This symmetry is preserved throughout the pH range investigated.

Figs. 3 and 4 show respectively the ^{1}H and ^{13}C NMR chemical shifts of **L2** as a function of pH.

At pH 9.3, where the $[H\mathbf{L2}]^+$ species prevails in solution (Fig. 2), the resonances of the hydrogens H(2) as well as those of the methyl group H(1), in the α-position with respect to N(1), experience a downfield shift with respect to the ^{1}H spectrum at pH 11.6, while the other signals do not shift appreciably (see Fig. 3). This suggests that the first proton which binds to the macrocycle is located on the methylated nitrogen N(1). This hypothesis is confirmed by the ^{13}C spectrum recorded at this pH, which shows that the signal of the carbon atom C3 shifts upfield (Fig. 4), in good agreement with the β-shift reported for protonation of polyamines.[18] It has been found that, in polyazaparacyclophanes, the benzylic nitrogens are the preferential protonation sites.[17a,19] On the other hand, in **L2** the first protonation occurs on the N(1) methylated nitrogen. Such different behaviour may be ascribed to the formation of a hydrogen bond network involving the protonated N(1) nitrogen and the N(2) and N(8) amine groups of the piperazine units, as actually shown by the crystal structure of the $[H_5\mathbf{L2}]^{5+}$ cation (see below). Formation of hydrogen bonds leads to a stabilization of the monoprotonated $[H\mathbf{L2}]^+$ species and may also explain the higher value of the first protonation constant for **L2** (log K = 9.81, Table 1) in comparison with **L1** (log K = 8.93), where the first protonation step involves the benzylic nitrogens. It is to be noted that, although the macrocycle has all tertiary nitrogens, its first protonation constant is very similar to that of ethylenediamine (log K = 9.9), which contains primary amine groups. This feature confirms the influence of molecular topology on the basicity characteristics of this kind of macrocycles.

In the pH range 9–7.5, where the $[H_2\mathbf{L2}]^{2+}$ and $[H_3\mathbf{L2}]^{3+}$ spe-

Table 2 ^{1}H and ^{13}C NMR chemical shift (ppm) of **L2** in aqueous solution at pH 11.6 (integration in parentheses)

C(1)	C(2)	C(3)	C(4), C(13)	C(5)	C(6)	C(7)[a]	C(8)	C(9)	C(10)	C(11)	C(12)	C(14)	C(15)
43.4	53.6	55.3	52.9	52.5	62.8	136.4	131.2	131.6	137.5	62.2	43.4	54.8	43.1
(1 C)	(2 C)	(2 C)	(6 C)	(4 C)	(2 C)		(4 C)	(4 C)		(2 C)	(2 C)	(2 C)	(1 C)

H(1)	H(2), H(3), H(4), H(5)	H(6)	H(8), H(9)	H(11)	H(12)	H(13), H(14)	H(15)
1.98	2.46	3.48	7.28	3.45	2.22	2.37	2.15
(s, 3 H)	(m, 24 H)	(s, 4 H)	(s, 8 H)	(s, 4 H)	(s, 6 H)	(m, 8 H)	(s, 3 H)

[a] Integrations of signals of quaternary carbons have been omitted.

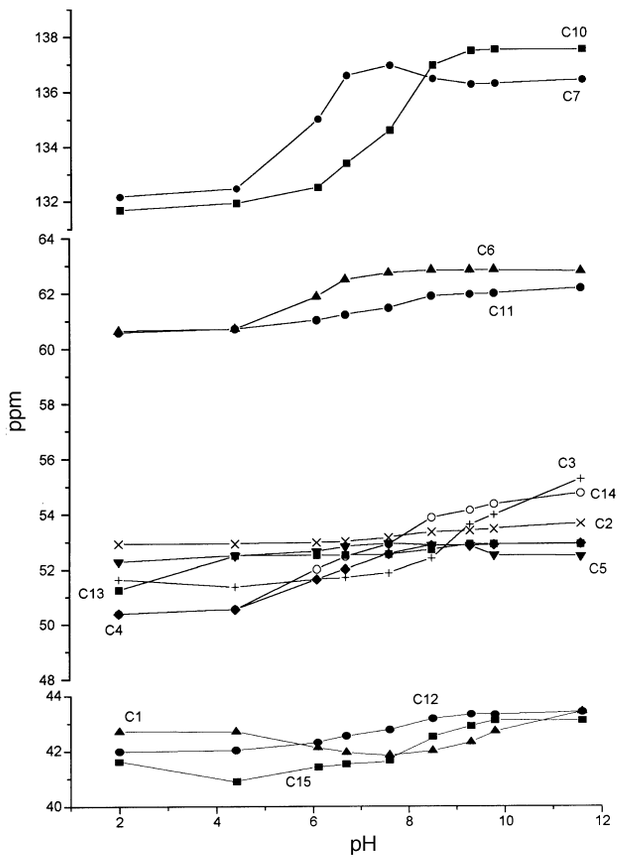

Fig. 4 Experimental ^{13}C NMR chemical shifts of **L2** as a function of pH. (The signals of the aromatic carbons 8 and 9 have been omitted for clarity. Their chemical shifts do not change significatively in the pH range investigated.)

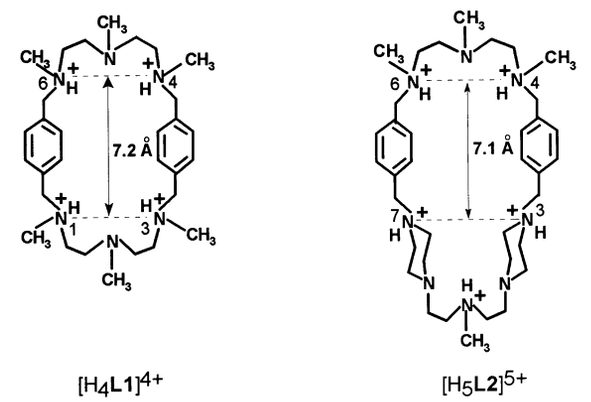

Fig. 5 Protonation sites in $[H_4\mathbf{L1}]^{4+}$ and $[H_5\mathbf{L2}]^{5+}$

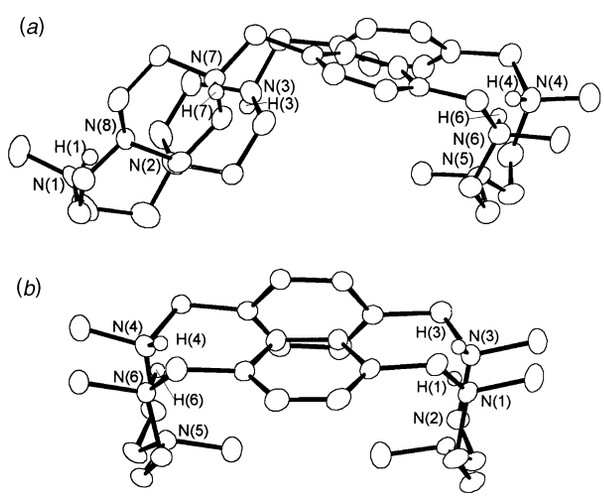

Fig. 6 ORTEP drawings of the $[H_5\mathbf{L2}]^{5+}$ (*a*) and $[H_4\mathbf{L1}]^{4+}$ (*b*) cations (labels of carbon atoms have been omitted for clarity)

cies are formed in solution, the signals of the hydrogens H11, H12 and H13, in the α-position with respect to N(4) and N(6), as well as those of H(5) and H(6), in the α-position with respect to N(3) and N(7), exhibit a marked downfield shift. In the same pH range, the resonances of the carbon atoms C(14) and C(10), in the β position with respect to N(4) and N(6), as well as the signals of C(4) and C(7), in the β position with respect to N(3) and N(7) shift upfield. These spectral data indicate that in the $[H_3\mathbf{L2}]^{3+}$ species two protons are shared by the four benzylic nitrogens N(3), N(4), N(6) and N(7). The same trend is shown by the ^{1}H and ^{13}C NMR spectra recorded at pH ≤ 4.4, where the only species present in solution is the pentaprotonated $[H_5\mathbf{L2}]^{5+}$ species (Fig. 2). In other words, in the pH range 9–4.4, four protons bind to the four nitrogen atoms N(3), N(4), N(6) and N(7). Consequently, in the pentaprotonated $[H_5\mathbf{L2}]^{5+}$ species, four of the five acidic protons are located on the benzylic nitrogens and one on the methylated nitrogen atom N(1), as shown in Fig. 5. Since the protons occupy alternate positions, separated from each other either by the aromatic rings or the unprotonated N(2), N(5) and N(8) nitrogens, such a disposition would mean a minimum in electrostatic repulsions.

Actually, this distribution of acidic protons in the $[H_5\mathbf{L2}]^{5+}$ species is confirmed by the crystal structure of the $[H_5\mathbf{L2}](ClO_4)_5\cdot 1.5H_2O$ salt.

Finally, the sixth protonation takes place on the nitrogen N(5), as confirmed by the sharp downfield shift experienced by the hydrogen atoms H(14) and H(15) in the ^{1}H spectrum at pH 2 (Fig. 3) and by the upfield shift of C(13) in the ^{13}C NMR spectra at the same pH (Fig. 4).

Description of the molecular structure of $[H_5\mathbf{L2}](ClO_4)_5\cdot 1.5H_2O$

The molecular structure consists of $[H_5\mathbf{L2}]^{5+}$ cations, perchlorate anions and water solvent molecules. An ORTEP[20] drawing of the protonated ligand, with atom labelling, is shown in Fig. 6(*a*).

The overall conformation of the macrocycle is boat-shaped. The five acidic protons are located on the N(1), N(3), N(4), N(6) and N(7) nitrogen atoms. The amine groups N(1), N(2), N(4), N(5), N(6) and N(8) are in *endo* configuration while N(3) and N(7) are in the *exo* configuration, due to the chair conformation of the piperazine rings. As a consequence, the N(4)–H(4) and the N(6)–H(6) bonds point almost inside the

Table 3 Stability constants (log K) and $\Delta G°$ values for the formation of the ATP and ADP (A) adducts with **L1**, determined by means of potentiometric measurements in 0.15 mol dm^{-3} NaCl at 298.1 K

	ATP		ADP	
Reaction	log K	$\Delta G°$/kJ mol^{-1}	log K	$\Delta G°$/kJ mol^{-1}
H_2**L1** + A = H_2**L1**A [a]	3.6 [b]	20.5	3.1	17.7
H_3**L1** + A = H_3**L1**A	4.2	24.9	3.5	20.0
H_4**L1** + A = H_4**L1**A	4.8	27.4	3.8	21.7
H_4**L1** + HA = H_5**L1**A	4.9	27.9	3.8	21.7
H_4**L1** + H_2A = H_6**L1**A	4.9	27.9	3.6	20.5

[a] Charges omitted for clarity. [b] Standard deviations on the stability constants are ±0.1.

macrocyclic cavity, while N(3)–H(3) and N(7)–H(7) face outside the macrocyclic cavity. Close comparisons can be found in the crystal structure of the $[H_4\mathbf{L1}](ClO_4)_4$ salt.[17a] Similarly to the present case, in the $[H_4\mathbf{L1}]^{4+}$ the four acidic protons are located on the benzylic nitrogens [Fig. 6(*b*)].[17a] Moreover, the conformation of the triaza-subunit in $[H_5\mathbf{L2}]^{5+}$ is almost the same as that found in $[H_4\mathbf{L1}]^{4+}$. In the $[H_5\mathbf{L2}]^{5+}$ cation the N(4)–H(4) and N(6)–H(6) bonds are orientated as the N(1)–H(1) and N(3)–H(3) bonds in $[H_4\mathbf{L1}]^{4+}$, while the two N(3)–H(3) and N(7)–H(7) bonds are faced outside the macrocyclic cavity, in an almost opposite direction with respect to the N(4)–H(4) and N(6)–H(6) bonds, due to the conformation of the piperazine rings.

Considering the N(1) protonation site, H(1) gives rise to intramolecular H-bonds with the nitrogen atoms in an *endo* configuration of the piperazine rings [H(1)···N(8) 2.49(7), H(1)···N(2) 2.68(7) Å]. Further hydrogen bonding interactions are found between the unprotonated N(5) nitrogen and N(4)–H(4) and N(6)–H(6) [H(4)···N(5) 2.36(7), H(6)···N(5) 2.48(9) Å].

In both $[H_5\mathbf{L2}]^{5+}$ and $[H_4\mathbf{L1}]^{4+}$ structures the two aromatic rings are not coplanar; in $[H_4\mathbf{L1}]^{4+}$ the dihedral angle is 74.2°, while in $[H_5\mathbf{L2}]^{5+}$ it is 38.3(3)°.

Finally, intermolecular H-bonds are formed between the acidic protons H(1), H(3) and H(7) and the oxygen atoms of water molecules or perchlorate anions. A hydrogen-bond network is also given by water–water and water–perchlorate interactions. Details about these interactions are reported within the Supplementary Material.†

ATP and ADP Binding

Binding of ATP and ADP by **L1** has been studied by means of potentiometric measurements and ^{1}H and ^{31}P NMR. Protonation of the receptor **L1** gives charged species which enables **L1** to form stable complexes with anionic forms of ATP and ADP in aqueous solution. The species formed, their stability constants and the corresponding $\Delta G°$ values are reported in Table 3. **L1** forms complexed species of the type $[H_n\mathbf{L1}ATP]^{(n-4)+}$ and $[H_n\mathbf{L1}ADP]^{(n-3)+}$, the protonation degree, n, varying from 2 to 6 in both cases. The $[H_2\mathbf{L1}ATP]^{2-}$, $[H_3\mathbf{L1}ATP]^{-}$ and $[H_4\mathbf{L1}ATP]$ species, as well as the corresponding ADP complexes, are formed from alkaline to slightly acidic pH (pH 9–6). In this pH range protons bind to the macrocycle, while ATP and ADP are in their unprotonated polycharged form. The stability of the complexes increases with the protonation degree of the complexes up to $n = 4$. An increasing number of protonated polyammonium functions increases the receptor's ability to give charge–charge and hydrogen bonding interactions with the anionic substrates. Protonation degrees over 4 imply the protonation of nucleotides and the stability constants for the penta- and hexa-protonated adducts are very similar to those found for the tetraprotonated $[H_4\mathbf{L1}ATP]$ and $[H_4\mathbf{L1}ADP]^{+}$ species. Finally, for the same protonation degree, the ADP complexes show a somewhat lower stability in comparison with the ATP adducts. This behaviour can be reasonably ascribed to weaker charge–charge interactions in the ADP complexes, due to lower negative charge on this anion.

Interaction with nucleotides have been also analysed by means of ^{1}H and ^{31}P NMR. ^{1}H NMR spectra were recorded on D_2O solutions containing **L1** and ATP or ADP in equimolecular ratio at pH 5 (at this pH the nucleotides are almost completely complexed by the receptor) and the complexation induced ^{1}H chemical shifts (CIS) are reported in Table 4. For both substrates upfield displacements of *ca*. 0.1 ppm are observed for the resonances of the adenine protons H(2), H(8) and for the anomeric proton H(1′) of the nucleotides, as well as for the aromatic protons R7 of **L1**. These CIS values may be indicative of π-stacking interactions involving the adenine moiety of nucleotides. Minor changes are observed for the protons of the sugar moiety as well as for aliphatic protons of the receptor. Remarkably higher CIS values for the hydrogens of the adenine moiety are usually found when π-stacking interactions give an important contribution to complex formation, as in the case of inclusion of the nucleobase into the receptor cavity.[5c] In the present case the low CIS values for the adenine signals indicate that the nucleobase cannot be included in the too small cavity of the receptor. Most likely, π-stacking takes place from outside the cavity.

On the other hand, complexation of the substrates produces variations in the ^{31}P chemical shifts, as already observed for analogous complexes with polyammonium macrocyclic receptors.[12,13] For instance, ^{31}P NMR spectra recorded for solutions containing **L1** and ATP or ADP at pH 5 show downfield shifts of 1.1 and 0.1 ppm for the signals of P_β and P_α of ADP, while P_γ, P_β and P_α of ATP shift 0.6, 0.1 and 0.4 ppm with respect to the corresponding signals of the free nucleotides at the same pH.

These results indicate that the formation of the adducts takes place mainly *via* the polyphosphate chains of ADP or ATP. Electrostatic forces play an important role in the complex formation between such charged species, although hydrogen bonding and π-stacking interactions may give further contributions to the stability of the adducts.

The rigidity of the cyclic framework makes $[H_4\mathbf{L1}]^{4+}$ a highly preorganized receptor for anion binding. Close comparisons can be found in the ditopic macrocycle [24]aneN_6O_2.[12,14] This receptor is composed by two triamine moieties separated by CH_2–CH_2–O–CH_2–CH_2 chains. Each triamine unit can bind two protons in aqueous solution, giving a tetraprotonated species $[H_4[24]aneN_6O_2]^{4+}$, which coordinates ATP or ADP. It has been found that the tetracharged receptor assumes an elongated boat-shaped conformation achieving a spatial charge matching between protonated nitrogens and the polyphosphate chains of ATP or ADP.[12,14] Such a mode of interaction can also be proposed in our case. Fig. 7 shows a proposed structure for the $[H_4\mathbf{L1}ADP]^{+}$ complex. A similar mode of interaction, involving two contiguous phosphate groups, can be also proposed for ATP binding. In particular, in the $[H_4\mathbf{L1}]^{4+}$ cation the separation between the two protonated triamine moieties. [7.2 Å, calculated from the X-ray crystal structure as the distance between the N(1)···N(3) middle point and the N(4)···N(6) middle point, as shown in Fig. 5] is very close to that proposed for optimal binding of ATP or ADP by the tetraprotonated form of [24]aneN_6O_2.[14]

$[H_4\mathbf{L1}]^{4+}$ exhibits a convergent orientation of the four acidic protons [see Figs. 6(*b*) and 7] which allows both the binding moieties to participate in substrate binding through the formation of several contacts with the phosphate groups. In other words preorganization of the receptor and complementarity between the binding sites of the polyammonium guest (N–H^+

† Supplementary data (SUPPL. NO. 57215, 3 pp.) are available from the British Library. For details of the Supplementary Publications Scheme see 'Instructions for Authors', *J. Chem. Soc., Perkin Trans. 2*, Issue 1, 1997.

Table 4 ^{1}H NMR shifts (δ, ppm) for the **L1** adducts with ATP and ADP and complexation-induced ^{1}H NMR chemical shifts (CIS, ppm) for selected protons, measured in D_2O solution at pH 5, 298 K

		R2	R3	R5	R7	H(8)	H(2)	H(1′)	H(5′)
ATP	δ	2.72[a]	3.24	4.45	7.70	8.40	8.14	5.99	4.31
	CIS	−0.03[b]	−0.02	+0.02	−0.14	−0.09	−0.08	−0.12	+0.08
ADP	δ	2.78	3.27	4.46	7.75	8.44	8.20	6.07	4.30
	CIS +	0.03	+0.01	+0.03	−0.09	−0.12	−0.1	−0.13	+0.08

[a] From measurements in D_2O solution at pH 5, 298 K, with a receptor : substrate 1 : 1 molar ratio. Under these conditions the complexation degrees are 87 and 82% for ATP and ADP respectively. [b] CIS (for 100% complexation) calculated based on equilibrium constants from Table 3.

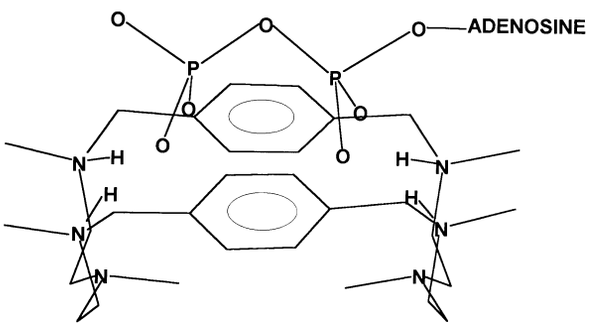

Fig. 7 Schematic representation for the interaction between $[H_4\mathbf{L1}]^{4+}$ and ADP (π-stacking interactions are not represented)

groups) and nucleotides (phosphate groups) may explain the rather high complex stability. Schneider and co-workers carried out a great deal of work in order to quantify the electrostatic contribution to the overall free energy change of a single ion contact.[5] The contribution of a single contact, or salt bridge, was found to be 5 ± 1 kJ mol^{-1}. Adopting this criterion, the $\Delta G°$ value of 21.7 kJ mol^{-1} found for the $[H_4\mathbf{L1}ADP]^+$ species (Table 3) may indicate that four salt bridges are involved in the formation of this complex, lending confidence to the proposed interaction mode sketched in Fig. 7. Similarly, in the case of the $[H_4\mathbf{L1}ATP]$ adduct the $\Delta G°$ value may account for the formation of five ionic contacts.

L2 shows a molecular architecture similar to **L1**, composed of two polyamine subunits linked by aromatic spacers. The presence of aromatic moieties, the short ethylenic chains connecting the amine groups, nitrogen methylation and the piperazine rings give rise to a stiffened macrocyclic backbone. Protonation of the receptor further increases the rigidity of the structure. In the $[H_5\mathbf{L2}]^{5+}$ species the four benzylic nitrogens are protonated, both in solution and in the solid state, resulting in a disposition of charges similar to that found in $[H_4\mathbf{L1}]^{4+}$. The distance between the two binding subunits in $[H_5\mathbf{L2}]^{5+}$ is 7.1 Å [calculated from the X-ray crystal structure as the distance between the N(3)···N(7) middle point and the N(4)···N(6) middle point, as shown in Fig. 5], almost equal to that previously found in $[H_4\mathbf{L1}]^{4+}$. This very similar spatial distribution of charges in the two cations leads one to suppose that a similar charge–charge matching between the phosphate chain of ATP or ADP and the receptor can also be achieved in $[H_5\mathbf{L2}]^{5+}$. Nevertheless, no interaction between ATP, ADP and the receptor is observed by means of potentiometry.‡ Furthermore, both ^{1}H and ^{31}P NMR spectra carried out on solutions containing the receptor and ADP or ATP in equimolecular ratios at various pH values do not reveal complexation of the substrates.

The crystal structure of the $[H_5\mathbf{L2}]^{5+}$ cation can be used to give a tentative explanation of such different behaviour with respect to $[H_4\mathbf{L1}]^{4+}$. In $[H_5\mathbf{L2}]^{5+}$ the N–H$^+$ benzylic groups of the two polyaza subunits adopt a divergent orientation and so would not be suitably positioned for simultaneous binding. As shown in Fig. 6, the conformation of the triaza-subunit is almost equal to that found in the $[H_4\mathbf{L1}]^{4+}$ cation and the N(4)–H(4) and N(6)–H(6) bonds in $[H_5\mathbf{L2}]^{5+}$ are orientated as the N(1)–H(1) and N(3)–H(3) bonds in $[H_4\mathbf{L1}]^{4+}$. On the other hand, in $[H_5\mathbf{L2}]^{5+}$ the two N(3)–H(3) and N(7)–H(7) bonds are faced in almost opposite directions with respect to the N(4)–H(4) and N(6)–H(6) bonds, due to the conformation of the piperazine rings. This divergent orientation of the two pairs of N–H$^+$ bonds in the $[H_5\mathbf{L2}]^{5+}$ species prevents the two polyamine subunits from forming simultaneously contacts with the phosphate groups of nucleotides, *i.e.* only two N–H$^+$ groups are available for the formation of salt bridges with the phosphate chains of the receptors. Apparently, these two binding contacts are not sufficient to give rise to a detectable interaction in our experiments.

It seems likely that a prerequisite to achieving a strong host–guest interaction in aqueous solution with this type of receptor is the presence of spatially separated N–H$^+$ binding sites suitably directed to interact with the complementary polyphosphate chain of the substrate.

Experimental

Synthesis of the compounds

The macrocycle **L1** was obtained as already described.[17b]

6,13,15,18-Tetramethyl-6,13,15,18-tetraaza-1(1,4),11(1,4)-dibenzena-3(1,4),9(1,4)-dipiperazina-cyclodecanonaphane octahydrochloride (L2·8HCl·3H$_2$O)

Bis(2-piperazinylethyl)methylamine triperchlorate[22] (4 g, 0.0072 mol) and K_2CO_3 (30 g, 0.216 mol) were suspended in refluxing CH_3CN (300 ml). To this mixture, a solution of 1,4,7-trimethyl-1,7-bis[*p*-(α-chloromethylbenzyl)]-1,4,7-triazaheptane trihydrochloride[17b] (3.8 g, 0.0072 mol) in CH_3CN (100 ml) was added dropwise in 7 h. After the addition was completed, the suspension was refluxed for 8 h and then filtered. The filtrate was vacuum evaporated to yield the crude product which was chromatographed on neutral alumina (activity II/III) eluting with a 100 : 1.5 $CHCl_3$–MeOH mixture. The eluted fractions were collected and evaporated to dryness to afford pure **L2** as a yellowish oil. The octahydrochloride salt **L2**·8HCl·3H$_2$O was obtained by adding 37% HCl to an ethanolic solution of **L2**. Yield 1.8 g (26%) (Found: C, 45.1; H, 8.0; N, 11.6. Calc. for $C_{36}H_{74}N_8Cl_8O_3$: C, 45.48; H, 7.85; N, 11.79%).

Crystals of $[H_5\mathbf{L2}](ClO_4)_5\cdot 1.5H_2O$, suitable for X-ray analysis, were obtained by slow evaporation at room temp. of an aqueous solution of **L2** at pH 4.

EMF measurements

The protonation constants of **L2** and the formation constants of the ATP and ADP complexes with **L1** were determined by potentiometry. All the potentiometric measurements were carried out in 0.15 mol dm^{-3} NaCl at 298.1 ± 0.1 K, in the pH range 2.5–11, by using the equipment that has been previously described.[23] The reference electrode was a Ag/AgCl electrode in saturated KCl solution. The glass electrode was calibrated as

‡ The species selection criterion used in this work has been reported in ref. 21, footnote 18. By using this criterion, species whose concentration is less than 5% throughout the pH range investigated are commonly rejected.

a hydrogen concentration probe by titrating known amounts of HCl with CO_2-free NaOH solutions and determining the equivalent point by the Gran's method[24] which allows determination of the standard potential E^o, and the ionic product of water ($pK_w = 13.73 \pm 0.01$). At least three measurements (*ca.* 100 experimental points each) were performed for each system. The computer program SUPERQUAD[25] was used to calculate the protonation constants and the stability constants of the ATP and ADP complexes from EMF data. The titration curves for each system were treated either as a single set or as separated entities without significant variations in the values of the basicity constants.

NMR spectroscopy

200.0 MHz ^{1}H and 50.32 MHz ^{13}C NMR spectra in D_2O solutions at different pH values were recorded at 298 K on a Bruker AC-200 spectrometer. In ^{1}H NMR spectra peak positions are reported relative to HOD at 4.75 ppm. Dioxane was used as reference standard in ^{13}C NMR spectra ($\delta = 67.4$ ppm). ^{1}H–^{1}H and ^{1}H–^{13}C 2D correlation experiments were performed to assign the signals. Small amounts of 0.01 mol dm^{-3} NaOD or DCl solutions were added to a solution of **L1**·6HCl·1.5H_2O or **L2**·8HCl·3H_2O to adjust the pD. The pH was calculated from the measured pD values using pH = pD − 0.40.[26] The ^{31}P NMR spectra were recorded at 81.01 MHz on a Bruker AC-200 spectrometer. Chemical shifts are relative to an external reference of 85% H_3PO_4.

Crystal data for $[H_5L2](ClO_4)_5 \cdot 1.5H_2O$

$C_{36}H_{68}Cl_5N_8O_{21.5}$, $M_w = 1134.23$, triclinic, $a = 8.87(1)$, $b = 15.388(6)$, $c = 20.476(7)$ Å, $\alpha = 102.80(3)°$, $\beta = 93.43(5)°$, $\gamma = 101.41(6)°$, $V = 2656(3)$ Å^3 (by least-squares refinement of diffractometer angles of 25 carefully centred reflections, $\lambda = 1.5418$ Å), space group $P\bar{1}$, $Z = 2$, $D_c = 1.418$ g cm^{-3}, parallelepiped-shaped colourless crystals (approximate dimensions 0.2 × 0.2 × 0.4 mm), μ(Cu-Kα) = 3.193 mm^{-1}.

Data collection and processing[27]

Enraf-Nonius CAD4 X-ray diffractometer. $\theta - 2\theta$ scan mode with θ scan width = 0.5 + 0.15 tan θ, θ speed variable. Graphite monochromatized Cu-Kα radiation; 5683 reflections measured ($3.02 < \theta < 49.97°$, $\pm h$, $\pm k$, l). Two standard reflections monitored: no loss of intensity observed. Lorentz and polarization effects correction applied.

Structure analysis and refinement§

Direct methods were used and absorption corrections were applied after structure resolution. Refinement was by full-matrix least-squares with all the non-hydrogen atoms anisotropic; aliphatic and aromatic hydrogen atoms were placed in calculated positions (final anisotropic displacement parameters $U = 0.082$ and 0.05 Å^2, respectively). A high degree of disorder was found for the oxygen atoms bound to Cl(4) and Cl(5). Six oxygen atoms were introduced around both Cl(4) and Cl(5). Their population parameters were fixed in such a way that the sum was 4 for each perchlorate. A disordered oxygen atom of a water molecule was introduced with a population parameter 0.5. All the acidic hydrogen atoms were located in a ΔF map and isotropically refined. The function minimized was $\Sigma w(|F_o|^2 - |F_c|^2)^2$, with the weighting scheme calculated in agreement with the resolution program (weighting factors 0.19 and 1.78). 702 parameters were refined, and final agreement factors of $R = 0.0803$ [3126 unique reflections with $I > 2\sigma(I)$] and $wR^2 = 0.2895$ were obtained. The programs used and source of atomic scattering factors and anomalous dispersion corrections are given in ref. 27. Atomic coordinates, bond lengths and angles, and thermal parameters have been deposited at the Cambridge Crystallographic Data Centre (CCDC). For details of the deposition scheme, see 'Instructions for Authors', *J. Chem. Soc., Perkin Trans. 2*, 1997, Issue 1. Any request to the CCDC for this material should quote the full literature citation and the reference number 188/55.

§ Computer used: DEX-486 DX.

Acknowledgements

Financial support by Italian Ministero dell'Università e della Ricerca Scientifica e Tecnologica (quota 40%) and by the Italian Research Council (CNR) is gratefully acknowledged.

References

1 J. Rebek, Jr., *Acc. Chem. Res.*, 1990, **23**, 399.
2 A. D. Hamilton, in *Inclusion Phenomena and Molecular Recognition*, ed. J. L. Atwood, Plenum, New York, 1990, p. 57.
3 K. T. Chapman and W. C. Still, *J. Am. Chem. Soc.*, 1989, **111**, 3075.
4 (*a*) F. P. Schmidtchen, *Tetrahedron Lett.*, 1989, **116**, 6081; (*b*) F. P. Schmidtchen, *Top. Curr. Chem.*, 1991, **161**, 101; (*c*) K. Worm, F. P. Schmidtchen, A. Schier, A. Shäfer and M. Hesse, *Angew. Chem., Int. Ed. Engl.*, 1994, **33**, 360.
5 (*a*) H. J. Schneider, *Angew. Chem.*, 1991, **30**, 1417; (*b*) H. J. Schneider, T. Schiestel and P. Zimmermann, *J. Am. Chem. Soc.*, 1992, **114**, 7698; (*c*) H. J. Schneider, T. Blatter, B. Palm, U. Pfingstag, V. Rüdiger and I. Theis, *J. Am. Chem. Soc.*, 1992, **114**, 7704; (*d*) A. V. Eliseev and H. J. Schneider, *J. Am. Chem. Soc.*, 1994, **116**, 6081 and references therein.
6 H. Fuuta, D. Magda and J. L. Sessler, *J. Am. Chem. Soc.*, 1991, **113**, 978.
7 Y. Murakami, J. Kikuchi, T. Ohno, O. Hayashida and M. Kojima, *J. Am. Chem. Soc.*, 1990, **112**, 7672.
8 F. Vögtle, H. Sieger and W. M. Müller, *Top. Curr. Chem.*, 1981, **98**, 107.
9 F. M. Menger and K. K. Catlin, *Angew. Chem., Int. Ed. Engl.*, 1995, **34**, 2147.
10 M. T. Reetz, C. M. Niemeyer and K. Harms, *Angew. Chem., Int. Ed. Engl.*, 1991, **30**, 1472.
11 (*a*) A. Bencini, A. Bianchi, M. I. Burguette, E. Garcia-España, S. V. Luis and J. A. Ramirez, *J. Am. Chem. Soc.*, 1992, **114**, 1919; (*b*) A. Bencini, A. Bianchi, M. I. Burguette, P. Dapporto, A. Domenech, E. Garcia-España, S. V. Luis, P. Paoli and J. A. Ramirez, *J. Chem. Soc., Perkin Trans. 2*, 1994, 569; (*c*) A. Bencini, A. Bianchi, C. Giorgi, V. Fusi, E. Garcia-España, J. M. Llinares, J. A. Ramirez, P. Paoletti and B. Valtancoli, *Inorg. Chem.*, 1996, **35**, 1114.
12 (*a*) M. W. Hosseini and J.-M. Lehn, *Helv. Chim. Acta*, 1987, **70**, 1312; (*b*) M. W. Hosseini, J.-M. Lehn, L. Maggiora, M. P. Mertes and K. B. Mertes, *J. Am. Chem. Soc.*, 1987, **109**, 537; (*c*) M. W. Hosseini, A. J. Blaker and J.-M. Lehn, *J. Am. Chem. Soc.*, 1990, **112**, 3896; (*d*) M. Dhaenens, J.-M. Lehn and J. P. Vigneron, *J. Chem. Soc., Perkin Trans. 2*, 1993, 1379.
13 (*a*) J. A. Aguilar, E. Garcia-España, J. A. Guerrero, S. V. Luis, J. M. Llinares, J. F. Miravet, J. A. Ramirez and C. Soriano, *J. Chem. Soc., Chem. Commun.*, 1995, 2237; (*b*) J. A. Aguilar, E. Garcia-España, J. A. Guerrero, S. V. Luis, J. M. Llinares, J. F. Miravet, J. A. Ramirez and C. Soriano, *Inorg. Chim. Acta*, 1996, **246**, 287.
14 M. P. Mertes and K. B. Mertes, *Acc. Chem. Res.*, 1990, **23**, 413 and references therein.
15 H. Chen, S. Ogo and R. H. Fish, *J. Am. Chem. Soc.*, 1996, **118**, 4993.
16 O. F. Shall and G. W. Gokel, *J. Org. Chem.*, 1996, **61**, 1449.
17 (*a*) C. Bazzicalupi, A. Bencini, A. Bianchi, V. Fusi, G. Giorgi, P. Paoletti, A. Stefani and B. Valtancoli, *J. Chem. Soc., Perkin Trans. 2*, 1995, 1379; (*b*) C. Bazzicalupi, A. Bencini, A. Bianchi, V. Fusi, C. Giorgi, P. Paoletti, S. Stefani and B. Valtancoli, *Inorg. Chem.*, 1995, **34**, 552.
18 (*a*) J. C. Batchelor, J. H. Prestegard, R. J. Cushly and S. R. Lipsy, *J. Am. Chem. Soc.*, 1973, **95**, 6558; (*b*) A. R. Quirt, J. R. Lyerla, I. R. Peat, J. S. Cohen, W. R. Reynold and M. F. Freedman, *J. Am. Chem. Soc.*, 1974, **96**, 570; (*c*) J. C. Batchelor, *J. Am. Chem. Soc.*, 1975, **97**, 3410; (*d*) J. E. Sarnessky, H. L. Suprenant, F. K. Molen and C. N. Reilley, *Anal. Chem.*, 1975, **47**, 2116.
19 (*a*) A. Andres, M. I. Burguete, E. Garcia-España, S. V. Luis, J. F. Miravet and C. Soriano, *J. Chem. Soc., Perkin Trans. 2*, 1993, 749; (*b*) A. Bianchi, B. Escuder, E. Garcia-España, S. V. Luis, V. Marcelino, J. F. Miravet and J. A. Ramirez, *J. Chem. Soc., Perkin Trans. 2*, 1994, 1253; (*c*) J. A. Aguilar, E. Garcia-España, J. A. Guerrero, J. M. Llinares, J. A. Ramirez, C. Soriano, A. Bianchi, L. Ferrini and V. Fusi, *J. Chem. Soc., Dalton Trans.*, 1996, 239.
20 C. K. Johnson, ORTEP, Report ORNL-3794; Oak Ridge National Laboratory, Oak Ridge, TN, 1971.

21 A. Bencini, A. Bianchi, E. Garcia-España, M. Micheloni and P. Paoletti, *Inorg. Chem.*, 1988, **27**, 176.
22 C. Bazzicalupi, A. Bencini, V. Fusi, M. Micheloni, P. Paoletti and B. Valtancoli, *J. Org. Chem.*, 1994, **59**, 7508.
23 A. Bianchi, L. Bologni, P. Dapporto, M. Micheloni and P. Paoletti, *Inorg. Chem.*, 1984, **23**, 1201.
24 (*a*) G. Gran, *Analyst* (*London*), 1952, **77**, 661; (*b*) F. J. C. Rossotti and H. Rossotti, *J. Chem. Educ.*, 1965, **42**, 375.
25 P. Grans, A. Sabatini and A. Vacca, *J. Chem. Soc., Dalton Trans.*, 1985, 1195.
26 A. K. Covington, M. Paabo, R. A. Robinson and R. G. Bates, *Anal. Chem.*, 1968, **40**, 700.
27 (*a*) SIR 92: A. Altomare, G. Cascarano, C. Giacovazzo and A. Guagliardi, *J. Appl. Crystallogr.*, 1993, **26**, 343; (*b*) DIFABS: N. Walker and D. D. Stuart, *Acta Crystallogr., Sect. A*, 1983, **39**, 158; (*c*) SHELXL-93, G. M. Sheldrick, SHELXL-93, Göttingen, 1993; (*d*) *International Tables for X-Ray Crystallography*, Kynoch, Birmingham, England, 1974, vol. IV.

Paper 6/05481A
Received 6*th August* 1996
Accepted 20*th November* 1996